Search and rescue: tackling antibiotic resistance with chemistry

Wade, N.

Chapter 2

Mechanistic investigations of metallo-ß-lactamase inhibitors: strong zinc binding is not required for potent enzyme inhibition

Parts of this chapter can be found in:

N. Wade, K. H. M. E. Tehrani, N. C. Brüchle, M. J. van Haren, V. Mashayekhi and N. I. Martin, *ChemMedChem*, 2021, **16**, 1651 – 1659.

1. Introduction

Antibiotics revolutionized health care in the mid 20th century, and they continue to be a cornerstone of modern medicine. Among all classes of antibiotics, the β-lactams are the most widely used, with broad-spectrum penicillins and cephalosporins accounting for 55% of antibiotics consumed in 2010.[1] Unfortunately, the widespread use of β-lactams over the past decades has led to the emergence of bacterial pathogens with resistance to all classes of β-lactam antibiotics used today.[2] The most notable mode of β-lactam resistance is via the production of β-lactamase enzymes that catalyse the opening of the β-lactam ring. The β-lactamases can be mechanistically divided into two types; serine β-lactamases (SBLs, Ambler class A, C and D) and metallo-β-lactamases (MBLs, Ambler class B).[3] Inhibitors of the SBLs have been successfully developed and include the clinically used clavulanic acid, sulbactam, tazobactam, and the most recent avibactam and vaborbactam.[4] MBLs, however, are mechanistically different from SBLs and rely on active site Zn^{2+} ion(s) to activate a water molecule that in turn hydrolyses the β-lactam ring.[5] This mechanistic difference means that clinically used SBL inhibitors have little-to-no effect on MBLs. Currently, there are no clinically approved MBL inhibitors.

Among the known MBLs the so-called New Delhi metallo-β-lactamase (NDM) and imipenemase (IMP) enzymes are among the best studied and confer resistance to a wide range of β-lactam antibiotics. The active site of both the NDM and IMP families are conserved and contain one Zn^{2+} ion coordinated to three histidine side chains and a second Zn^{2+} coordinated by histidine, aspartic acid, and cysteine residues.[6,7] While NDM and IMP enzymes share structural similarities, their primary amino acid sequences differ significantly leading to differences in both their catalytic efficiency and sensitivity to small molecule inhibitors.[8–11]

The present lack of any clinically approved MBL inhibitor emphasizes the need for investigation and innovation in this area. Ideally, an MBL inhibitor would be administered as part of a combination therapy with the capacity to restore the activity of a β-lactam antibiotic against otherwise resistant bacteria expressing an MBL. While no MBL inhibitor has yet been granted approval for use in humans, a wide range of inhibitors, spanning a diversity of structural and mechanistic features, have been reported in both the scientific and patent literature in recent years. The structures of these reported MBL inhibitors contain a wide variety

of pharmacophores that can deactivate the MBLs most often by either zinc-sequestration (i.e. "zinc stripping") or by coordination to zinc as part of the compound's interaction within the MBL active site.[12] Strong metal chelators that actively strip zinc ions from the MBL active site can effectively deactivate the enzyme's ability to hydrolyse the β-lactam ring.[13] Alternatively, there are also small molecule MBL inhibitors that instead of removing zinc from the enzyme, coordinate the metal ion within the active site and in doing so displace the activated water molecule which in turn blocks catalysis.[7,14]

Developing inhibitors that effectively cover all MBL sub-types is a challenge with many factors to consider. As the MBLs are metallo-enzymes, searching for inhibitors with the capacity to chelate or bind the active site zinc ions would appear to be an obvious strategy. However, there is a significant risk involved with the use of zinc binding compounds *in vivo* given the possibility of off-target effects related to the many other metallo-enzymes involved in human metabolism.[15,16] Among the earliest reported MBL inhibitors were various thiol and thio-carbonyl compounds which demonstrated potent *in vitro* enzyme inhibition for a range of MBLs.[17] However, the rapid oxidation of thiols to homo- and hetero-disulphides in biological systems can negatively affect their clinical success.[18,19] Ideally, an MBL inhibitor should be stable enough for use *in vivo* and also not interfere with the binding of biologically relevant metals needed for the function of other vital metallo-enzymes.

Given the above-mentioned challenges associated with MBL-inhibitor discovery, it is crucial to understand the physicochemical (specifically metal-binding) properties of MBL-inhibitors in order to clarify their inhibitory mechanism, as well as their likelihood of having off-target effects if administered *in vivo*. To this end, we surveyed the recent scientific and patent literature and assembled a broad panel of 13 structurally distinct MBL inhibitors for the purpose of a comparative study. Specifically, we set out to: 1) Establish the relative inhibitory potency of these MBL inhibitors in a directly comparative manner (i.e. using the same biochemical assay) by determining the IC_{50} values for each inhibitor against purified NDM-1 and IMP-1; 2) Assess the metal binding properties of the MBL inhibitors using isothermal titration calorimetry (ITC) to quantify their affinity for the biologically relevant divalent cations Zn^{2+}, Ca^{2+}, and Mg^{2+}; and 3) Assess the ability of these MBL inhibitors to synergize with a last resort carbapenem antibiotic (meropenem) in resensitising an *E. coli* strain expressing NDM-1. **Figure 1** provides an overview of the structures of the MBL inhibitors selected for the present study. The strong metal chelators, 1,4,7,10-tetraazacyclododecane-

1,4,7,10-tetraacetic acid (DOTA) **1**, ethylenediaminetetraacetic acid (EDTA) **2** and ethylene glycol-bis(2-aminoethylether)-*N,N,N′,N′*-tetraacetic acid (EGTA) **3** are all known to have a high affinity for divalent cations making them ideal candidates to study as inhibitors that inactivate MBLs by zinc stripping.[10,11,20] The pyridine based *N,N,N′,N′*-tetrakis(2-pyridylmethyl)ethylenediamine (TPEN) **4** and di-(2-picolyl)amine **5** were also included as they have been described as MBL inhibitors with the ability to bind zinc.[21] Another category of compounds included were the *N*-heterocycle carboxylates thiazolidine-2,4-dicarboxylic acid **6**, picolinic acid **7,** and dipicolinic acid (DPA) **8** which have been shown to inhibit MBL enzymes such as NDM-1 and CphA.[22,23] As representative members of the thiol-based MBL inhibitors, dimercaprol **9**, L-captopril **10**, and thiomandelic acid **11** were selected.[14,22,24–27] In addition, compounds **12** and **13** were included as both were recently reported in the patent literature as displaying potent MBL inhibiton.[28,29] Distinct from the other MBL inhibitors chosen for this study, compounds **12** and **13** are the result of high-throughput screening and medicinal chemistry efforts specifically aimed at identifying MBL inhibitors. Compound **12** comes from a library of inhibitors all containing an indole-2-carboxylate core, shown to have potent NDM-1 inhibition.[28] Compound **13** demonstrates promising *in vitro* inhibition of NDM-1 and VIM-2 and is under development by the biopharmaceutical company Antabio. A recent co-crystal structure of compound **13** in complex with VIM-2 shows that the compound interacts with the MBL active site via Zn^{2+} coordination by the carboxylate moiety and thiazole nitrogen atom in addition to interacting with active site residues.[30]

In light of the growing interest in MBL inhibitor development we here provide a comparative analysis of the biochemical, biophysical, and biological properties of a representative set of MBL inhibitors. Notably, our study provides for a direct assessment of the relative activity of these inhibitors against the NDM and IMP type enzymes. A number of studies published in recent years have used a variety of assay conditions to establish MBL inhibitor potency and synergy. In contrast, our investigation employs the exact same assay conditions in assessing the inhibitory activities of the MBL inhibitors studied and in doing so provides for a reliable comparison. In addition, in determining the metal binding affinities of the MBL inhibitors here studied, we reveal the somewhat surprisingly finding that tight zinc binding is by no means a prerequisite for potent enzyme inhibition. Notably, at the time of writing a manuscript appeared from Crowder and co-workers describing the use of equilibrium dialyses with metal analyses, native state electrospray ionization mass spectrometry (ESI-MS), and UV-Vis spectrophotometry to compare the activity and mechanism of various MBL inhibitors towards

the Verona integron-encoded metallo-β-lactamase 2 (VIM-2).[31] The techniques used and results reported in the Crowder group's study with VIM-2 are complimentary to the methods we use and support well the findings here described in our comparative analysis of MBL inhibitors towards the NDM and IMP classes.

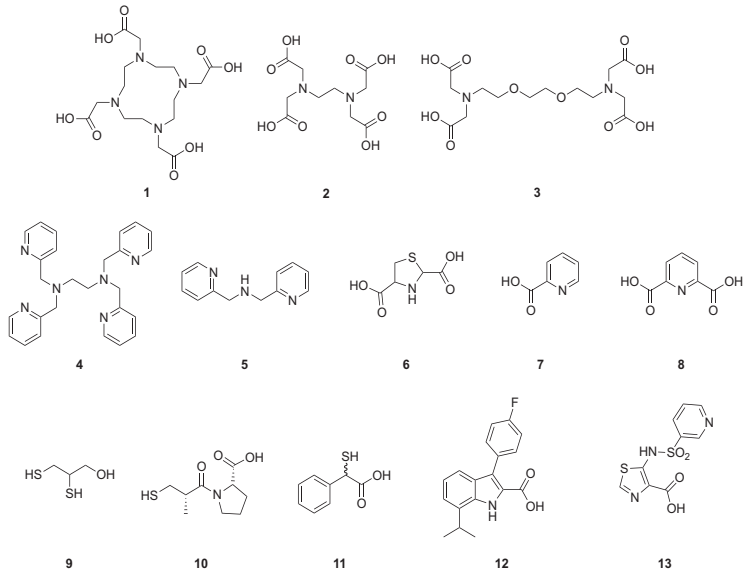

Figure 1. Structures of inhibitors: heavy metal chelators (**1-4**), pyridine-based chelators (**4-5**), N-heterocyclic carboxylic acids (**6-8**), thiols (**9-11**) and HTS derived inhibitors (**12-13**).

2. Results and Discussion

2.1 Acquiring MBL inhibitors

Among the MBL inhibitors used in the present study, compounds **1-11** are commercially available, while **12** and **13** are not and were therefore synthesized. Compound **12** was prepared according to patent literature by the route shown in Scheme 1A.[28] Briefly, ethyl acetoacetate was alkylated with 4-fluorobenzyl bromide to yield the expected substituted *β*-ketoester. The next step involved the *in situ* diazotization of 2-isopropyaniline, which, in the presence of the substituted *β*-ketoester intermediate from the previous step, resulted in hydrazone formation (Japp-Klingemann reaction) followed by spontaneous cyclization under acidic conditions to form the indole scaffold. Ester hydrolysis in turn gave compound **12** (experimental details provided in accompanying supplemental information). The synthesis of compound **13** was achieved following a modified protocol from the patent literature and is illustrated in Scheme

1B.[29] The route started by cyclization of 4-methoxybenzyl isothiocyanate with *t*-butyl isocyanoacetate to yield the thiazole core. Subsequent reaction of this intermediate with pyridine-3-sulfonyl chloride afforded the corresponding sulfonamide. Notably, yields for the formation of the sulfonamide were best when starting from the PMB protected thiazole intermediate and using potassium bis(trimethylsilyl)-amine as a base. Following sulphonamide formation, global deprotection using acidic conditions led to compound **13** (experimental details provided in accompanying supplemental information).

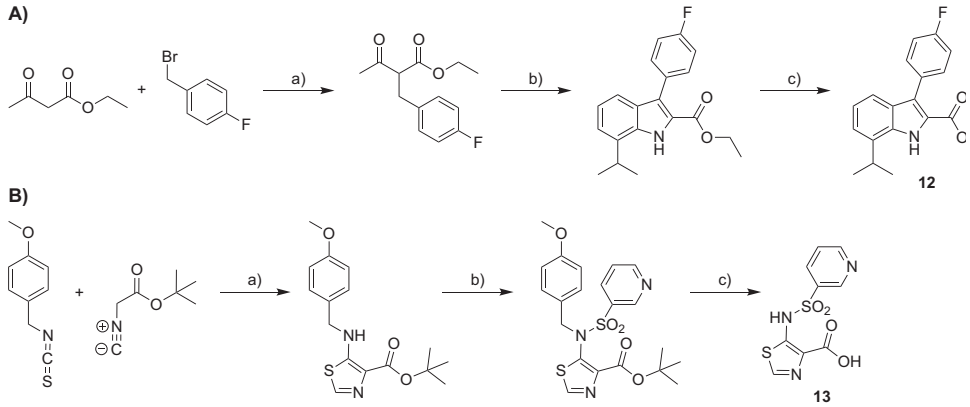

Scheme 1. A) Synthesis of **12** *a) ethyl acetoacetate, 4-fluorobenzylbromide, potassium tert-butoxide, tert-butanol, THF; b) i. 2-isopropylaniline, sodium nitrate, conc. HCl, MeCN; ii. KOH, H_2O, EtOH, iii. HCl, EtOH; c) NaOH, THF, EtOH.* B) Synthesis of **13** *a) potassium tert-butoxide, THF; b) pyridine-3-sulfonyl chloride, potassium bis(trimethylsilyl)-amide, DMF/THF; c) TFA.*

2.2 Determining IC_{50} values against NDM-1 and IMP-1

With inhibitors **1-13** in hand, we next determined their half-maximal inhibitory concentrations (IC_{50} values) against purified NDM-1 and IMP-1 enzymes. For these assays, the fluorogenic cephalosporin substrate FC5 was synthesized and used as previously described.[32] The K_M and K_{cat} values for FC5 hydrolysis by NDM-1 corresponded with those previously found.[33] The results of this study, shown in **Table 1**, highlight differences between the compounds studied and their ability to inhibit the two enzymes. The metal chelating compounds **1-5** are particularly strong inhibitors of NDM-1 but are significantly less effective against IMP-1. The heterocyclic carboxylates **6-8** also showed NDM-1 selectivity among which DPA **8** was the most potent against both enzymes. Thiols **9-11** were found to have low- to sub-μM IC_{50} values against both NDM-1 and IMP-1. Among these, thiomandelic acid **11** was the most effective with IC_{50} values

of 3.2 and 0.02 μM against NDM-1 and IMP-1 respectively. Among the MBL-inhibitors selected from the recent patent literature, indole-carboxylate **12** showed an impressive potency activity against both NDM-1 and IMP-1 with IC_{50} values in the nM-range. Notably, while inhibitor **13** exhibited nM potency against NDM-1 it was found to be significantly less active towards IMP-1.

Table 1. IC_{50} values of the inhibitor against either NDM-1 or IMP-1

Compound	IC_{50}[a] (μM)	
	NDM-1	IMP-1
1	1.34 ± 0.06	>200
2	1.97 ± 0.06	>200
3	0.280 ± 0.016	>200
4	0.644 ± 0.245	109 ± 11.3
5	2.60 ± 0.17	116 ± 0.9
6	55.0 ± 5.92	>200
7	84.0 ± 7.25	>200
8	4.26 ± 0.28	15.2 ± 0.168
9	4.21 ± 0.40	2.19 ± 0.070
10	7.21 ± 0.88	3.48 ± 0.254
11	3.17 ± 0.06	0.023 ± 0.001
12	0.005 ± 0.002	0.140 ± 0.003
13	0.275 ± 0.029	>200

[a]The half-maximal inhibitory concentration values for each compound against NDM-1 and IMP-1 with FC5 used as the substrate.

2.3 Measuring dissociation constants of inhibitors to divalent cations

The ability of inhibitors **1-13** to bind the biologically relevant divalent cations Zn^{2+}, Ca^{2+}, and Mg^{2+} was next investigated. Understanding the metal binding properties of MBL inhibitors is of importance when considering their potential for therapeutic application given the high concentrations of free calcium and magnesium in the bloodstream, with values in adult humans of between 1.17-1.33 mM and 0.6-1.1 mM respectively.[34,35] These ions have the potential to 'distract' metal binding inhibitors from reaching the divalent zinc in the MBL targets. A range of methodologies and conditions have been used previously in evaluating the metal-binding

properties of some of the inhibitors included in our present study.[18,36–41] In an attempt to employ a more standardized approach, we used isothermal titration calorimetry to determine and compare the thermodynamic parameters governing the binding interaction between inhibitors **1-13** and the divalent cations Zn^{2+}, Ca^{2+}, and Mg^{2+}. Listed in **Table 2** are the values resulting from our ITC binding studies including: dissociation constant (K_d), enthalpy (ΔH), entropy ($-T\Delta S$), and Gibbs free energy (ΔG) (all binding thermograms are provided in the supporting information, see supplemental figure S2). In all cases, the MBL inhibitor evaluated showed much more potent zinc binding relative to either calcium or magnesium. Notably, the Zn-binding interaction of compounds **1-4** is very strong (estimated K_d <100 nM) precluding an accurate determination of their zinc binding constants based on the data obtained by ITC. The strong metal ion binding observed for **1-4** is in fact expected given the well-established capacity of these compounds to act as potent chelating agents all with K_d values of <1 nm as previously determined.[36,37] Also of note are compounds **5** and **9,** which exhibit an apparent two-step binding interaction with zinc. This behaviour can be rationalized as both compounds contain what appear to be two distinct metal binding sites. The heterocyclic carboxylates **6-8** were found to bind zinc with K_d values in the low μM to high nM range. Finally, compounds **10-13** were found to bind zinc rather weakly with K_d values for **11** and **13** in the μM range, while for **10** K_d is estimated in the mM range and as for **12**, no appreciable zinc binding could be measured with the ITC conditions used (even at concentration as high as 200 μM in the cell). When the binding interaction of *L*-captopril with NDM-1 was evaluated with ITC, a K_d value of 2.2 μM was measured.[42] This difference in binding affinity can be explained by the hydrogen binding interaction of captopril carboxylate as well as the hydrophobic interactions of captopril ring carbons with the different amino acid residues in the L10 and L3 loop of NDM-1 respectively.[14] The ITC results were particularly interesting in the case of compound **12** given that it was found to be the most potent inhibitor in our biochemical assays. These results clearly show that strong zinc binding is not a requirement for potent MBL inhibition. Also as noted above, ITC was also used to assess the binding of compounds **1-13** to Ca^{2+} and Mg^{2+}. While for some compounds appreciable binding to calcium and/or magnesium was detected, in all cases this binding was significantly weaker than that measured for Zn^{2+} (supplementary table S1 and S2).

Table 2. Binding of Zn^{2+} by MBL inhibitors **1-13** as assessed using ITC.

Compound	K_d (μM)	ΔH (kcal/mol)	-TΔS (kcal/mol)	ΔG (kcal/mol)
1	<100 nM[a]	-11.3 ± 0.09	-	-
2	<100 nM[a]	-8.80 ± 0.10	-	-
3	<100 nM[a]	-12.3 ± 0.06	-	-
4	<100 nM[a]	-12.0 ± 0.07	-	-
5	0.139 ± 0.062	-13 ± 0.08	3.61 ± 0.18	-9.41 ± 0.25
	1.47 ± 0.72	-2.49 ± 0.26	-5.54 ± 0.53	-8.02 ± 0.27
6	12.0 ± 0.3	-6.8 ± 0.07	0.06 ± 0.08	-6.7 ± 0.01
7	38.6 ± 2.5	-8.14 ± 0.12	2.11 ± 0.16	-6.02 ± 0.04
8	0.398 ± 0.045	-2.68 ± 0.12	-6.06 ± 0.57	-8.74 ± 0.69
9	0.069 ± 0.006	-27.97 ± 0.59	18.2 ± 0.56	-9.77 ± 0.05
	1.46 ± 0.41	-11.23 ± 0.78	3.26 ± 0.94	-7.99 ± 0.16
10	>1000[b]	-	-	-
11	27.2 ± 0.99	-10.6 ± 0.1	4.36 ± 0.08	-6.24 ± 0.02
12	NB[c]	-	-	-
13	60.6 ± 14.6	-16.7 ± 2.0	10.98 ± 2.14	-5.77 ± 0.15

[a]Under the experimental conditions used, K_d values below 100 nM cannot be accurately determined (only ΔH could be reliably measured). [b]Binding affinity was too low to accurately determine all of the parameters. [c]NB: No binding was observable or K_d too high to allow an accurate determination of the thermodynamic parameters associated with Zn^{2+} binding.

2.4 Synergy experiments with meropenem

Compounds **1-13** were also evaluated for their ability to synergize with the last-resort carbapenem antibiotic meropenem against a highly resistant (NDM-1 expressing) *E. coli* isolate. Prior to doing so, compounds **1-13** were first tested for any inherent antimicrobial activity against this strain. While compounds **1-13** generally showed no antibacterial activity at clinically relevant concentrations, TPEN **4** did exhibit an MIC of 125 μM. In addition, meropenem was also tested against the same strain confirming its resistance with a measured

MIC value of 64 μg/mL (see supplemental table S3 for full MIC data). The synergy assay performed was designed to establish the concentration of each MBL inhibitor required to reduce the MIC of meropenem by a factor of four (i.e. lowering the MIC from 64 μg/mL to 16 μg/mL). In doing so, each MBL inhibitor was administered as a dilution series in combination with meropenem (fixed at 16 μg/mL) to establish the lowest inhibitor concentration that resulted in bacterial killing when combined with meropenem at 16 μg/mL. The results from this assay are summarized in **Table 3** and reveal that most of the MBL inhibitors tested do not effectively synergize with meropenem against the highly drug resistant isolate used. Notable exceptions include compounds **2**, **4**, **12**, and **13** which were found to resensitise the NDM-1 expressing isolate to meropenem at 16 μg/mL at the lowest inhibitor concentration evaluated (15.6 μM). Using this data, we also calculated the fractional inhibitory concentration index value (FICI) of each inhibitor. Bearing in mind that an FICI of <0.5 indicates synergy, compounds **2**, **4**, **12**, and **13** stand out as the most potent synergisers in this study. Compounds **2** and **12** were chosen to carry out a full checkerboard assay with meropenem against *E. coli* RC89, the former as an example of a zinc stripping inhibitor and the latter discovered through medicinal chemistry efforts. The results show that both compounds show impressive synergy with meropenem, with FICI values of 0.031 and 0.063 for compounds **2** and **12** respectively (**Figure 2**).

2.5 Collating experimental results

Taken together, the IC_{50} values measured, the Zn^{2+} binding data, and the results of the antibacterial synergy assays obtained for MBL inhibitors **1-13** reveals some interesting trends. In the case of strong zinc chelators **1-4**, the compounds were found to be much more active against NDM-1 than IMP-1 in the biochemical enzyme inhibition assays. The finding that MBLs of the IMP class are less susceptible to zinc sequestration as a mode of inactivation, while the NDM type are sensitive to strong zinc binders, is in agreement with previous reports.[11,13,33] At present, a mechanistic explanation for this selectivity remains elusive. Among inhibitors **1**-**4**, EDTA **2** and TPEN **4** were also found to effectively synergize with meropenem against a highly resistant NDM-1 producing *E. coli* isolate. It is, however, notable that strong MBL inhibition does not guarantee synergy, as illustrated by DOTA **1** and EGTA **3** both of which were unable to resensitise the same bacteria to meropenem. This may be due to an inability of compounds **1** and **3** to effectively permeate the bacterial cell. The other compound evaluated in this series of chelators, compound **5,** can be viewed as a fragment of **4.** The reduced ability of compound **5** to synergize with meropenem or inhibit NDM-1 and IMP-1 compared

with **4** may be attributable to its lower binding affinity for Zn^{2+}, although the role of membrane permeability as an additional contributing factor to the synergistic activity cannot be excluded.

Table 3. Synergistic activity data of the MBL inhibitors **1-13**

Compound	$C_{MIC/4}$ (μM)[a,b]	FICI[c]
1	250	0.375
2	<15.6	<0.258
3	250	0.375
4	<15.6	<0.375
5	62.5	0.313
6	500	0.500
7	1000	>0.500
8	125	0.313
9	>1000	>0.500
10	500	0.500
11	500	0.500
12	<15.6	<0.258
13	<15.6	<0.258

[a]Values shown correspond to $C_{MIC/4}$ defined as the lowest concentration of the MBL inhibitor required to achieve a 4-fold reduction in the MIC of meropenem. [b]The bacterial isolate used was *E. coli* RC89, an NDM-1 expressing strain obtained from Utrecht Medical Centrum with an MIC for meropenem of 64 μg/mL. [c]FICI is the fractional inhibitory concentration index where a value of < 0.5 indicates synergy.

The heterocyclic carboxylates **6-8** performed reasonably well in the enzyme inhibition assays. Compounds **6** and **7** were found to be moderate inhibitors of NDM-1 with IC_{50} values of 55.0 and 84.0 μM respectively, but showed no activity toward IMP-1 (IC_{50} > 200 μM). By comparison, DPA (**8**) demonstrated reasonably potent inhibition of both enzymes with an IC_{50} value of 4.26 μM for NDM-1 and 15.2 μM for IMP-1. An explanation for these differences is suggested by the result of the ITC-based metal binding assays where DPA (**8**) was found to bind zinc with a K_d of 398 nM, nearly 100-fold lower than the value measured for **7** and 30-fold lower than **6**. Notably, DPA (**8**) also exhibits appreciable binding to Ca^{2+} (supplemental table S1), which would likely prove to be detrimental to its effectiveness against MBLs in more complex biological environments containing high levels of free calcium. Inhibitors **6-8** were

all found to be rather ineffective at synergizing with meropenem in preventing the growth of the NDM-1 expressing bacterial strain. While compounds **6** and **7** were essentially inactive in the synergy assays, when administered at 125 μM the well-studied DPA (**8**) did exhibit the capacity to reduce the MIC of meropenem 4-fold against the NDM-1-producing strain.

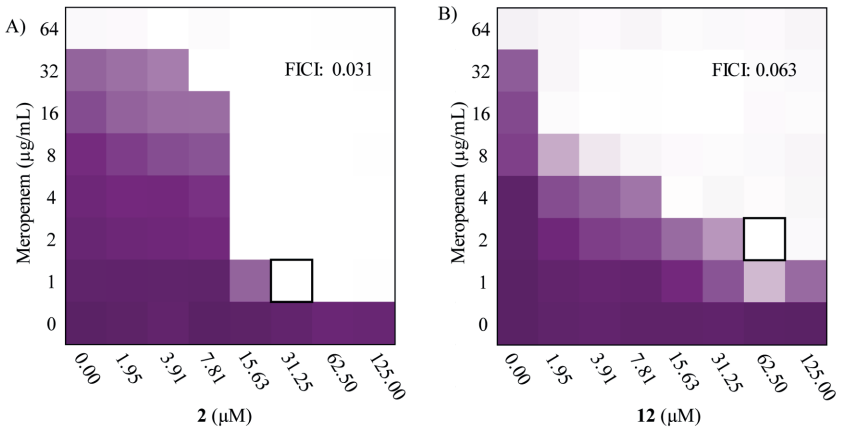

Figure 2. Checkerboard plots of the full synergy assay of compounds 2 and 12 in combination with meropenem against *E. coli* RC89. The mean optical density of the bacterial growth at 600 nm (OD_{600}) is shown as a colour gradient, purple signifying maximum bacterial growth and white as no growth. The combination of inhibitor and antibiotic which gave the lowest FICI is indicated with a black box.

For thiols **9-11**, a range of activities was observed. In the biochemical assays all three compounds showed moderate inhibition of NDM-1 (IC_{50} values in the low μM range) while against IMP-1 compound **11** was found to have an IC_{50} value of 23 nM, making it the most potent inhibitor among all of the compounds evaluated. Interestingly, the metal binding abilities of these compounds have little relation to the inhibitory activity. Dimercaprol **9** is a strong Zn^{2+} binder with an apparent two-step binding mode (K_d values in the low nM to low μM range). Conversely, thiomandelic **11** is a moderate zinc binder with a K_d of 27.2 μM while L-captopril **10** exhibited weak binding estimated to be in the mM range. In accordance with the biochemical assays, none of these compounds demonstrated particularly strong synergy with meropenem in preventing the growth of the NDM-1 expressing *E. coli* strain.

In comparison, the recently reported MBL inhibitors **12** and **13** were both found to strongly inhibit purified NDM-1 with IC_{50} values of 5 nM and 275 nM respectively - the most

potent NDM-1 inhibitors identified among the 13 compounds here studied. While moderate zinc binding was measured for compound **13** (K_d 60.6 μM) neither **12** nor **13** was found to bind the other metals tested. These findings suggest that these compounds may be less likely to elicit off-target effects arising from promiscuous metal binding. Interestingly, despite being a potent inhibitor of both NDM-1 and IMP-1, compound **12** demonstrated no detectable Zn^{2+} binding in the ITC assay used. This finding is particularly striking given that potent inhibition of NDM-1 and other MBLs has generally been associated with compounds that are able to sequester and/or strip zinc from the active site, such as EDTA **2**. It is, however, clear from our ITC studies that this is not the mode of MBL inhibition for compound **12**. These findings are even more notable given that **12** and **13** were also found to generally outperform known zinc sequestering MBL inhibitors in the synergy assay performed. Unlike most of the other inhibitors in this assay, **12** and **13** were found to be very effective in synergizing with meropenem against the NDM-1 expressing strain used. It is worth noting that **12** and **13** are the products of dedicated screening and optimization efforts aimed at identifying novel MBL inhibitors. Our findings reveal that there is indeed likely to be value in pursuing such focused approaches in the development of MBL inhibitors designed to specifically interact with the enzyme active site rather than relying explicitly on strong metal binding.

As mentioned earlier, a study from Crowder's group was published recently which used different biophysical approaches to evaluate the inhibitory mechanism of previously reported MBL inhibitors.[31] While the group has previous experience using the membrane dialysis assay of di-zinc MBLs as well as NMR and UV-Vis spectroscopy of cobalt-substituted MBLs, they introduced the use of native mass spectrometry to evaluate the mechanism of action of MBL inhibitors. The latter requires lower concentrations of enzymes and inhibitors (at low- to sub-μM levels) which is closer to the physiological conditions. Using this method, they detected the formation of zinc-free NDM-1 and ternary complex (enzyme-zinc-inhibitor) after incubation of NDM-1 with EDTA and captopril, respectively. However, as the authors admit, lack of internal standard precludes a quantitative assessment of enzyme interaction. Also notable was their findings on compound **13** when incubated with NDM-1 and VIM-2. Equilibrium dialysis experiments using both enzymes showed that, like captopril, compound **13** does not remove zinc from NDM-1 and VIM-2. In contrast, incubation with EDTA resulted in substantial depletion of zinc from NDM-1 and VIM-2. Interestingly, our ITC experiments adds more clarification to the matter as we found a moderate zinc affinity for **13** (K_d = 60 μM) while that of EDTA is estimated in the sub-nM level. Therefore, to the list of biochemical/biophysical set of assays proposed by Crowder's group,[42] we would like to add

the analysis of metal binding affinity of the newly designed inhibitors by ITC. Without the need to use enzymes, ITC gives a quick and early indication of the possibility of promiscuous metal binding by the inhibitor candidates. In addition, the trend that we observed in this study, indicates that inhibitors that display an extremely high affinity to bind zinc (K_d at the low-nM level or below) are unlikely to form a ternary complex with the MBL enzymes.

3. Conclusion

In recent years a variety of compounds have been described as possessing MBL inhibitory activity. However, in many cases sub-optimal selectivity (as for chelating agents) or stability (as for thiols) limits their potential for drug development. Moreover, active site heterogeneity among MBLs, as manifested in the differing sensitivities of NDM-1 and IMP-1 towards the chelating agents investigated in this study, point to challenges in the development of a broad-spectrum MBL inhibitor. As our investigations further reveal, the use of different biochemical and biophysical methods allows for a more complete understanding of the modes of action of MBL inhibitors. Such mechanistic insights are likely to be of importance in anticipating issues relating to *in vivo* safety and selectivity for MBL inhibitors in the early phases of drug development. Among the MBL inhibitors evaluated in our study, the indole carboxylate derivative **12** was found to exhibit an impressive combination of activity and selectivity. The compound effectively resensitises MBL-expressing bacteria to meropenem and is a potent and broad-spectrum MBL inhibitor with nM-range IC_{50} values against both NDM-1 and IMP-1. Furthermore, compound **12** shows no appreciable binding to free Zn^{2+}, Ca^{2+}, or Mg^{2+}. Taken together, these finding suggest that compound **12** and its analogues may present promising candidates for future drug development efforts aimed at overcoming MBL-expressing pathogens.

4. Materials and Methods

4.1 Materials

Commonly used solvents and reagents were purchased from either Sigma Aldrich or Combi-blocks. Compounds **1**, **2** and **5** were purchased from Sigma Aldrich. Compounds **6**, **7** and **8** were purchased from Combi-blocks. Compounds **3** and **9** were purchased from Alfa Aesar, compound **4** from Cayman Chemicals, and **10** from Acros. Compound **11** was prepared as previously described.[18] ^{1}H and ^{13}C NMR spectra were recorded on a Bruker AV-400 MHz or AV-500 MHz. Enzyme inhibition assays were carried out on a Tecan Spark plate reader. A PEAQ-ITC calorimeter (Malvern) was used to acquire the ITC thermograms. High resolution mass spectrometry (HRMS) analyses were performed on a Shimadzu Nexera X2 UHPLC system.

4.2 Compound synthesis

Compounds **12** and **13** were prepared according to published patent procedures with minor adjustments.[28,29]

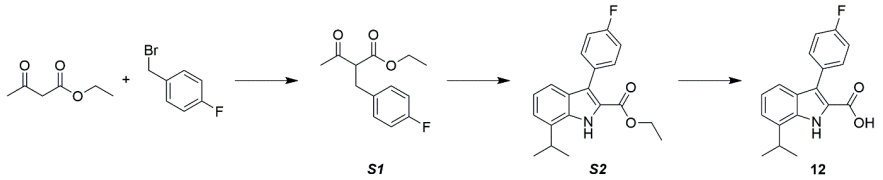

Scheme S1. Synthesis route used in preparation of compound **12**. The syntheses of intermediates **S1, S2** and final compound **12** were carried out as previously described.

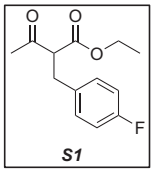

*Ethyl-2-(4-fluorobenzyl)-3-oxobutanoate (**S1**).* Potassium *tert*-butoxide (729 mg, 6.5 mmol, 1.3 eq) was suspended in dry THF (12 mL) and cooled to 0 °C before ethyl acetoacetate (822 µL, 6.5 mmol, 1.3 eq) and *tert*-butanol (47.8 µL, 0.5 mmol, 0.1 eq) were added. The reaction mixture was stirred for 0.5 h and then 4-fluorobenzyl bromide (623 µL, 5 mmol, 1 eq) was added dropwise. The reaction mixture was warmed to 70 °C until starting material was consumed as seen by TLC (DCM). The reaction was quenched with saturated aq. sodium bicarbonate (10 mL) and the aqueous layer was extracted with ethyl acetate (3x10 mL). The organic layers were combined, washed with brine, dried over sodium sulphate, concentrated and column purified over silica (PE with 5-

10% EtOAc) to obtain the desired product (619 mg, 52%). Analytical data in agreement with that previously reported.

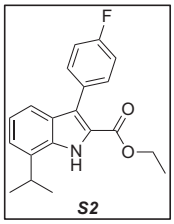

*Ethyl-3-(4-fluorophenyl)-7-isopropyl-1H-indole-2-carboxylate (**S2**).* In a mixture of acetonitrile (4 mL) and concentrated HCl (12M, 1.3 mL), 2-isopropylaniline (0.357 mL, 2.5 mmol, 1 eq) was dissolved and cooled to 0 °C. Sodium nitrate (189 mg, 2.75 mmol, 1.1 eq) dissolved in water (1.14 mL) was added dropwise and stirred for 0.25 h. In a separate reaction vessel, intermediate **S1** (600 mg, 2.5 mmol, 1 eq) was dissolved in an ice cooled mixture of potassium hydroxide (490 mg, 8.75 mmol, 3.5 eq), water (1.14 mL), and ethanol (2.86 mL) and stirred for 0.25 h. The first reaction mixture was then added dropwise to the second and stirred at room temperature for 16 h. When the starting material was consumed as monitored by TLC (PE with 10% EtOAc) the reaction mixture was partitioned between water (10 mL) and EtOAc (10 mL) and further extracted with ethyl acetate (3x10 mL). The combined organic layers were washed with brine and dried over sodium sulphate before being concentrated. The resulting residue was column purified (PE with 0-20% EtOAc) to obtain an oil (367 mg) that was directly dissolved in an ethanolic HCl solution (3.6 mL), prepared by adding acetyl chloride (0.48 mL) to ethanol (3.2 mL), and heated to reflux for 5 h. The reaction mixture was cooled to room temperature, concentrated, and partitioned between water (10 mL) and EtOAc (10 mL) and further extracted with ethyl acetate (3x10 mL). The combined organic phase was washed with brine, dried over sodium sulphate, and concentrated. The residue was column purified (PE with 0-20% EtOAc) to give the desired product (343.2 mg, 42% over two steps). Analytical data in agreement with that previously reported for the same compound series.

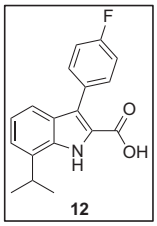

*3-(4-fluorophenyl)-7-isopropyl-1H-indole-2-carboxylic acid (**12**).* Intermediate **S2** (258 mg, 0.79 mmol) was dissolved in a mixture of THF (5 mL), ethanol (1 mL), and aq. sodium hydroxide (2M, 5 mL). The reaction was stirred for 16 h until the starting material was consumed as monitored by TLC (PE with 10% EtOAc) after which the reaction mixture was acidified to pH 1 with HCl (5M). The organic solvent was removed under vacuum and the aqueous layer freeze dried. The resulting powder was washed with cold water and dried under vacuum to give the final product (185 mg, 79%). ^{1}H NMR (400 MHz, MeOD) δ 7.52 (dd, J = 8.4, 5.5 Hz, 2H),

7.32 (d, J = 8.1 Hz, 1H), 7.22 (d, J = 7.2 Hz, 1H), 7.16 (t, J = 8.7 Hz, 2H), 7.07 (t, J = 7.6 Hz, 1H), 3.55 (sep, 1H), 1.40 (d, J = 6.8 Hz, 6H). ^{13}C NMR (101 MHz, CD_3OD) δ 163.48 (d, J = 43.6 Hz, 1C), 160.8, 145.5, 138.9, 132.8, 132.15 (d, J = 7.9 Hz, 2C), 129.6, 127.2, 123.4, 120.7, 120.5, 118.0, 114.1 (d, J = 21.5 Hz, 2C), 30.1, 22.0. HRMS (ESI$^+$): calcd. For $C_{18}H_{16}FNO_2$ $[M+H]^+$: 298.1238, found: 298.1208.

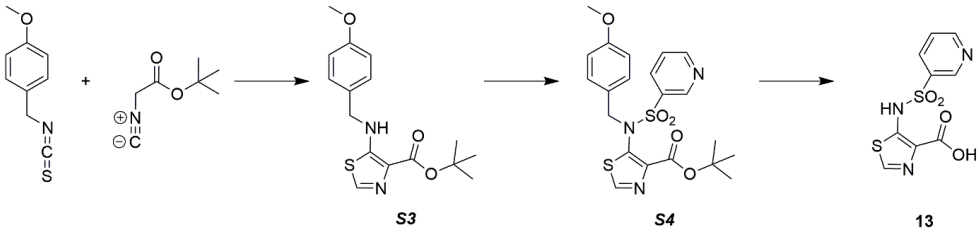

Scheme S2. Synthesis route used in preparation of compound **13**. The syntheses of intermediate **S3** and final compound **13** were carried out as previously described.

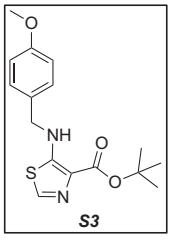

*tert-Butyl-5-((4-methoxybenzyl)amino)thiazole-4-carboxylate (**S3**).* To a suspension of potassium *tert*-butoxide (848 mg, 7.56 mmol, 1.1 eq) in dry THF (11 mL), a solution of *tert*-butyl isocyanoacetate (1 mL, 6.87 mmol, 1 eq) in dry THF (5 mL) was added dropwise. This solution was stirred for 10 minutes before a solution of 4-methoxybenzyl isothiocyanate (1.23 g, 6.87 mmol, 1 eq) in dry THF (5 mL) was added dropwise over 2h while stirring at room temperature. After 3 hours, the solution was poured into saturated sodium bicarbonate (25 mL) and extracted with EtOAc (3 x 25 mL). The combined organic layer was dried with sodium sulphate, concentrated under vacuum, and the residue applied to a silica column (PE with 12.5-20% EtOAc) to give the desired product (1.9 g, 86%). Analytical data in agreement with that previously reported.

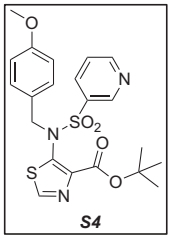

*tert-Butyl-5-(N-(4-methoxybenzyl)pyridine-3-sulfonamido)thiazole-4-carboxylate (**S4**)*. Intermediate **S3** (150 mg, 0.468 mmol, 1.0 eq) was dissolved in a DMF/THF mixture (5:2 ratio, 3 mL) and cooled to -78 °C before potassium bis-(trimethylsilyl)-amide (1.12 mmol, 1.0 M in THF, 2.4 eq) was added and stirred for 30 mins. Pyridine-3-sulfonyl chloride (62 µL, 0.515 mmol, 1.1 eq) was added and the mixture was brought to room

temperature and stirred for 16 h. The mixture was then poured into water (10 mL) and extracted with EtOAc (3 x 10 mL). The combined organic layers were dried with sodium sulphate, concentrated under vacuum, and the residue applied to a silica column (DCM with 0-5% MeOH as mobile phase) to give the product as an off-white powder (111 mg, 51%). ^{1}H NMR (500 MHz, $CDCl_3$) δ 8.89 (dd, J = 2.4, 0.8 Hz, 1H), 8.73 (dd, J = 4.9, 1.6 Hz, 1H), 8.52 (s, 1H), 7.93 (ddd, J = 8.1, 2.4, 1.6 Hz, 1H), 7.35 (ddd, J = 8.1, 4.9, 0.8 Hz, 1H), 7.05 – 7.02 (m, 2H), 6.72 – 6.69 (m, 2H), 4.86 (s, 2H), 3.69 (s, 3H), 1.41 (s, 9H). ^{13}C NMR (101 MHz, $CDCl_3$) δ 159.7, 159.3, 153.6, 152.0, 148.5, 143.0, 135.6, 135.4, 130.6, 126.3, 123.6, 114.1, 83.1, 55.7, 55.3, 28.1. 1. HRMS (ESI$^+$): calcd. For $C_{21}H_{23}N_3O_5S_2$ $[M+H]^+$: 462.1152, found: 462.1148.

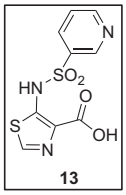

13

5-(pyridine-3-sulfonamido)thiazole-4-carboxylic acid (**13**). Intermediate **S4** (100 mg, 0.217 mmol) was dissolved in water (0.25 mL) and trifluoroacetic acid (3 mL). The reaction mixture was stirred for 1 h before the solvents were removed. The solid was triturated in diethyl ether and dried to give a brown powder (23 mg, 38%). ^{1}H NMR (400 MHz, DMSO) δ 8.93 (d, J = 2.4 Hz, 1H), 8.78 (dd, J = 4.9, 1.6 Hz, 1H), 8.48 (s, 1H), 8.17 (ddd, J = 8.1, 2.5, 1.6 Hz, 1H), 7.60 (ddd, J = 8.1, 4.9, 0.9 Hz, 1H). ^{13}C NMR (101 MHz, DMSO-d_6) δ 163.2, 153.4, 149.4, 147.2, 145.1, 137.6, 135.2, 131.2, 124.9. HRMS (ESI$^+$): calcd. For $C_9H_7N_3O_4S_2$ $[M+H]^+$: 285.9951, found: 285.9953.

4.3 Enzyme expression and purification

The plasmids containing NDM-1 and IMP-1 were provided by Prof. Christopher Schofield (Oxford University). To obtain IMP-1,[43] *Escherichia coli* BL21 (DE3) pLysS transformed with the plasmid was grown at 37 °C in 2 L of Luria-Bertani (LB) medium supplemented with kanamycin (50 µg/mL) to ensure selective growth. When the culture reached an optical density ($OD_{600\ nm}$) of 0.6, protein production was induced using 0.5 mM isopropyl-β-D-thiogalactopyranoside (IPTG). The cultures were grown for another 4 hours before the cells were harvested by centrifugation (4000 g) for 20 min and resuspended in 50 mM HEPES pH 7.0, 250 mM NaCl. The cells were lysed using sonication and centrifuged for 30 min at 30000 g. The supernatant was diluted with Buffer A (50 mM HEPES pH 7.0, 100 µM $ZnSO_4$) before being loaded onto a 1 mL HiTrap SP FF column (GE Healthcare) and subsequently eluted using a gradient of Buffer B (50 mM HEPES pH 7.0, 100 µM $ZnSO_4$, 1 M NaCl). The fractions were run on an SDS-PAGE gel and those containing IMP-1 were combined, concentrated using

spin filter columns (MilliPore) and loaded onto a size-exchange column (Superdex75 16/60; GE Healthcare). The fractions were once again assessed by SDS-PAGE and the pure fractions were combined and concentrated. The concentration of the protein was determined using a NanoDrop spectrometer. The expression and purification of NDM-1 was performed as previously described.[44]

4.4 Enzyme Inhibition assays

The half-maximal inhibitory concentration (IC_{50}) of each compound was determined against NDM-1 and IMP-1. The compounds were serially diluted (50 µL) and incubated with 25 µL of NDM-1 (40 pM) or IMP-1 (125 pM) for 15 min. Upon addition of FC5 substrate (0.5 µM for NDM-1 and 20 µM for IMP-1, 25 µL in each case), fluorescence was monitored over 25 cycles (λ_{ex} 380 nm, λ_{em} 460 nm) on a Tecan Spark plate reader. The initial velocity data was used to produce the IC_{50} curves using GraphPad prism 7 software. The buffer used in the experiments was 50 mM HEPES pH 7.2 containing 0.01% Triton X-100 and 1 µM zinc sulphate and the microplates used were µClear®, black half-area 96-well plate (Greiner Bio-one).

4.5 Isothermal Titration Calorimetry (ITC)

ITC experiments were performed using a MicroCal PEAQ-ITC Automated instrument (Malvern). The test compounds and metal salts were dissolved in Tris–HCl buffer (20 mM, pH 7.0). The solutions of divalent cations were titrated into a solution of the compound of interest via 19 aliquots of 2 µL (except the first injection which was 0.4 µL) with 150 s between injection. The only exceptions were dipicolylamine **5** and dimercaprol **9**, for which 32 and 28 aliquots of 1 µL (except the first injection of 0.4 µL) were titrated with 100 s between injections. The concentration of cations vs small molecules (ligands) for each titration is listed under each thermogram in supplemental Figure S2. All the experiments were performed at 25 °C in triplicate with the reference power set to 10 µcal/s. The data generated was analysed using the MicroCal PEAQ-ITC Analysis Software.

4.6 Antibacterial activity

Determination of minimum inhibitory concentration (MIC). Antibacterial assays were performed according to clinical and laboratory standards institute (CLSI) guidelines. Test compounds were serially diluted with Mueller-Hinton broth (MHB) in polypropylene 96-well plates (50 µL in each well). *E. coli* RC0089 (NDM-1) was inoculated into tryptic soy broth

(TSB) and incubated at 37 °C. Once the bacteria cells grew to an OD_{600} of 0.5, the suspension was diluted with MHB (final concentration 10^6 CFU/mL) and then added to the microplates containing the test compounds (50 µL to each well, final volume: 100 µL). After incubation at 37 °C for 16-20 h, the microplates were inspected for growth inhibition. MIC values were defined as the lowest concentration of the compound that prevented visible growth of bacteria. Synergy assay ($C_{MIC/4}$). The test compounds were serially diluted with MHB starting from a maximum concentration of 1000 µM (25 µL in each well). Meropenem (25 µL) was then added to the wells to achieve a final concentration of 16 µg/mL. *E. coli* RC0089 (NDM-1) was cultured and added to the microplates as described above (50 µL to each well, final volume: 100 µL). The $C_{MIC/4}$ value was defined as the lowest concentration of the inhibitor that prevented the visible growth of the bacteria when combined with meropenem at ¼ of its MIC. FICI values were established by applying the following formula where an FICI < 0.5 indicates synergy:

$$FICI = \frac{MIC_{Meropenem} \text{ in combination}}{MIC_{Meropenem} \text{ alone}} + \frac{MIC_{Inhibitor} \text{ in combination}}{MIC_{Inhibitor} \text{ alone}}$$

OD600 Checkerboard assay. The test compounds were serially diluted with MHB starting from a maximum concentration of X µM (25 µL in each well). Meropenem was serially diluted to 4x the final concentration before being added to the test compounds (25 µl). *E. coli* RC0089 was cultured and added to the microplates as described above (50 µL to each well, final volume: 100 µL). The microplates were then incubated at 37 °C with shaking. After XX h, the optical density of each well was measured using a Tecan Spark plate reader at 600 nm.

5. Supporting Information

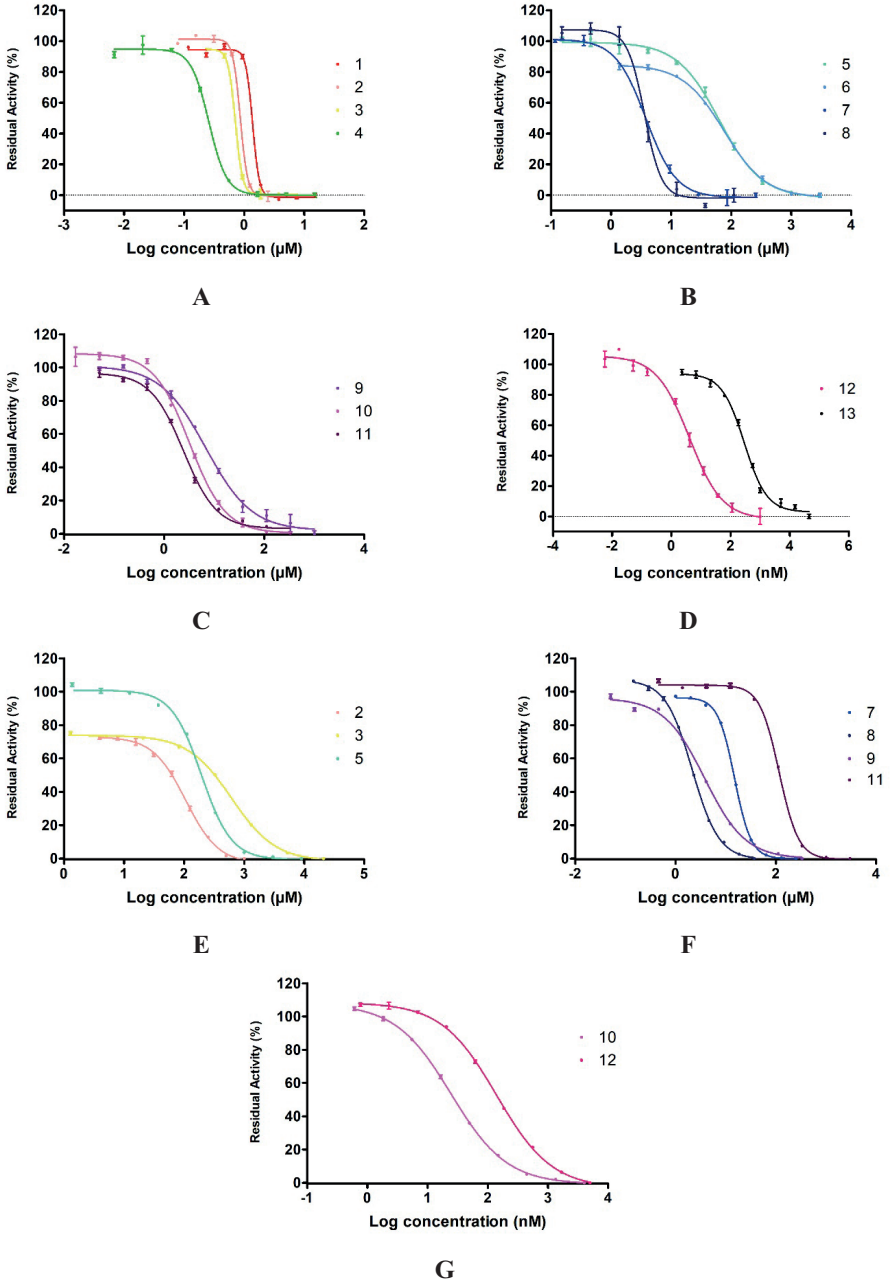

Figure S1. IC_{50} curves of compounds **1-13** against NDM-1 (**A**, **B**, **C**, **D**) and IMP-1 (**E**, **F**, **G**). All concentrations are in μM with the exception of compounds **12** and **13** which are in nM.

Table S1. Binding of Ca^{2+} by MBL inhibitors as assessed using isothermal titration calorimetry.

Compound[a]	K_d (μM)	ΔH (kcal/mol)	-TΔS (kcal/mol)	ΔG (kcal/mol)
1	<100nM[b]	-18.4 ± 0.09	-	-
2	<100nM[b]	-14.0 ± 0.04	-	-
3	<100nM[b]	-24.1 ± 0.06	-	-
8	38.5 ± 3.0	-4.04 ± 0.05	-1.98 ± 0.09	-6.02 ± 0.05

[a]The compounds excluded from the table showed no appreciable Ca^{2+} binding affinity. [b] Under the experimental conditions used, K_d values below 100 nM cannot be accurately determined (only ΔH could be reliably measured).

Table S2. Binding of Mg^{2+} by MBL inhibitors as assessed using isothermal titration calorimetry.

Compound[a]	K_d (μM)	ΔH (kcal/mol)	-TΔS (kcal/mol)	ΔG (kcal/mol)
2	1.94 ± 0.00	-2.61 ± 0.03	-5.18 ± 0.03	-7.79 ± 0.00

[a]The compounds excluded from the table showed no appreciable Mg^{2+} binding affinity.

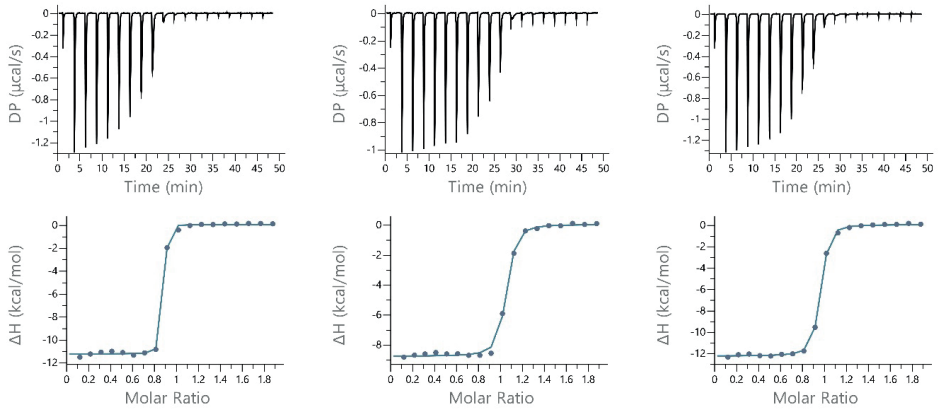

*Zn^{2+} (0.5 mM) : **1** (0.05 mM)* | *Zn^{2+} (0.5 mM) : **2** (0.05 mM)* | *Zn^{2+} (0.5 mM) : **3** (0.05 mM)*

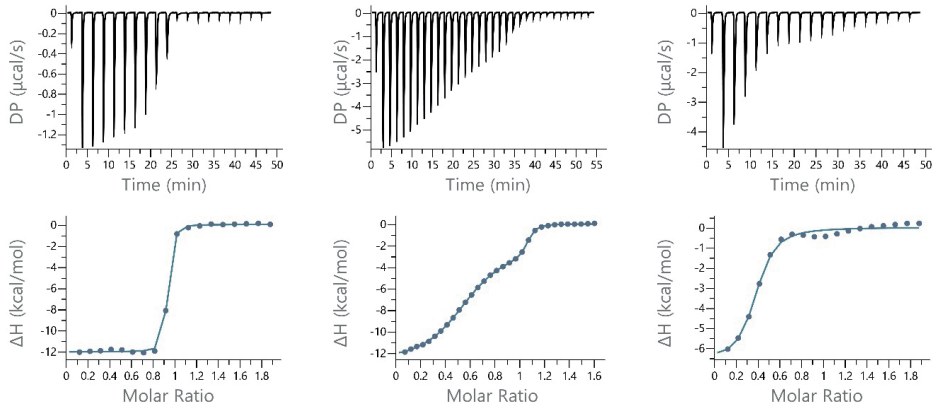

*Zn^{2+} (0.5 mM) : **4** (0.05 mM)* | *Zn^{2+} (5 mM) : **5** (0.5 mM)* | *Zn^{2+} (5 mM) : **6** (0.5 mM)*

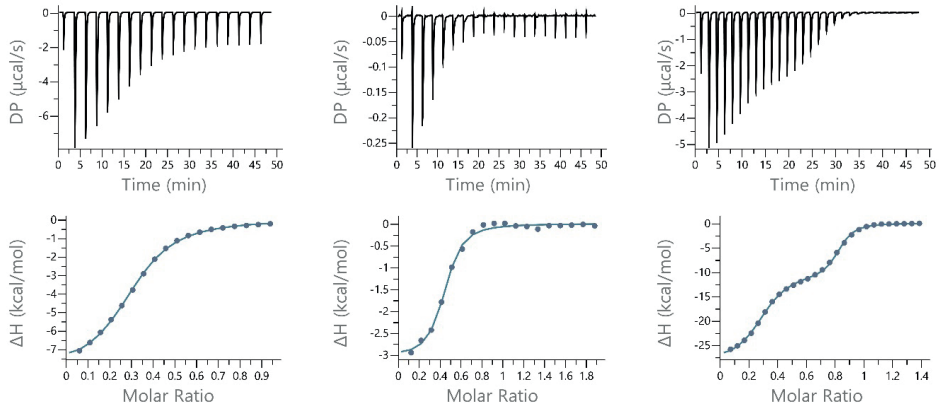

*Zn^{2+} (5 mM) : **7** (1 mM)* | *Zn^{2+} (0.5 mM) : **8** (0.05 mM)* | *Zn^{2+} (2 mM) : **9** (0.2 mM)*

Figure S2. *ITC thermograms*

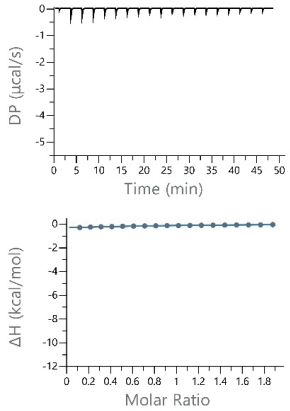

*Zn^{2+} (5 mM) : **10** (0.5 mM)*

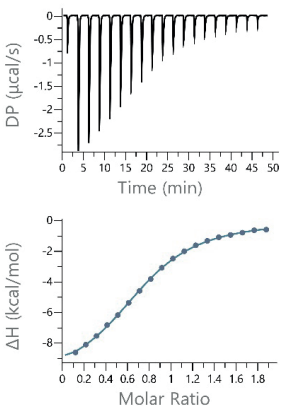

*Zn^{2+} (2 mM) : **11** (0.2 mM)*

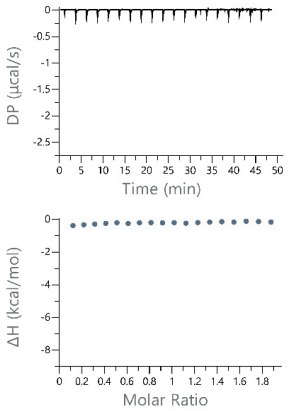

*Zn^{2+} (2 mM) : **12** (0.2 mM)*

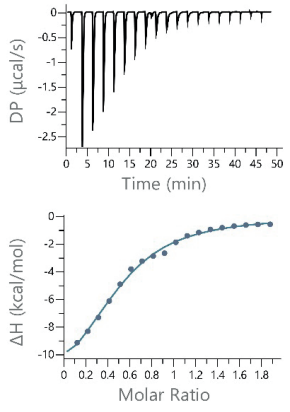

*Zn^{2+} (2 mM) : **13** (0.2 mM)*

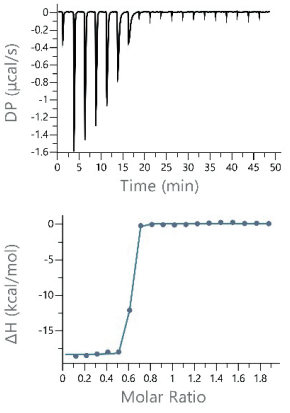

*Ca^{2+} (0.5 mM) : **1** (0.05 mM)*

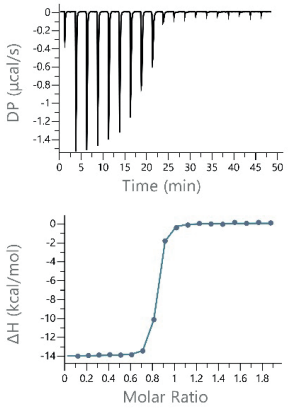

*Ca^{2+} (0.5 mM) : **2** (0.05 mM)*

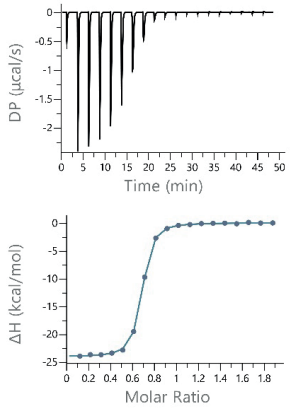

*Ca^{2+} (0.5 mM) : **3** (0.05 mM)*

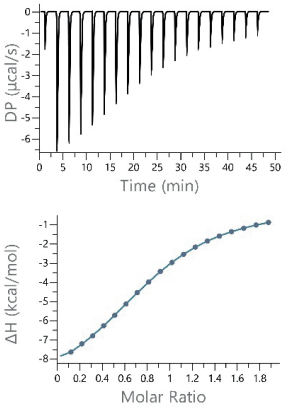

*Ca^{2+} (5 mM) : **4** (0.5 mM)*

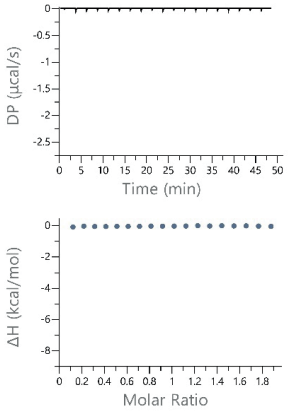

*Ca^{2+} (2 mM) : **5** (0.2 mM)*

Figure S2. *continued*

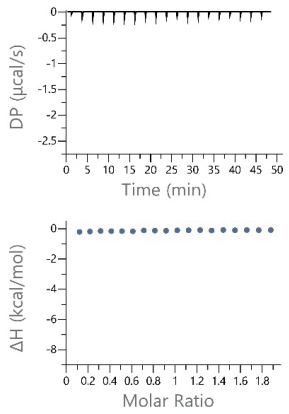

*Ca^{2+} (2 mM) : **6** (0.2 mM)*

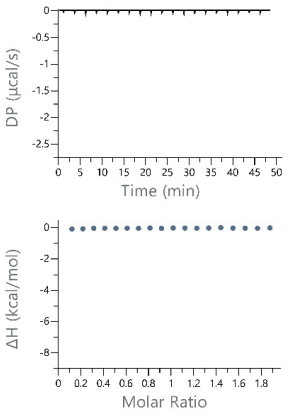

*Ca^{2+} (2 mM) : **7** (0.2 mM)*

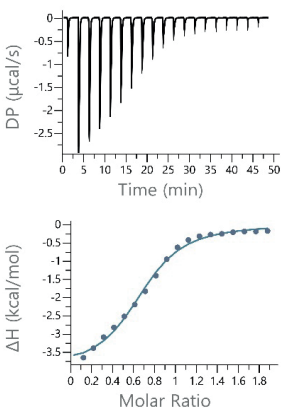

*Ca^{2+} (5 mM) : **8** (0.5 mM)*

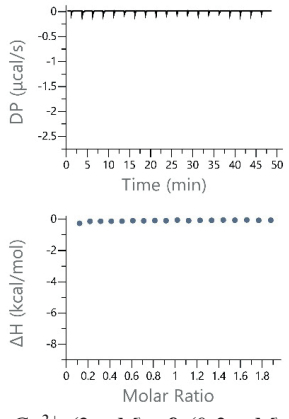

*Ca^{2+} (2 mM) : **9** (0.2 mM)*

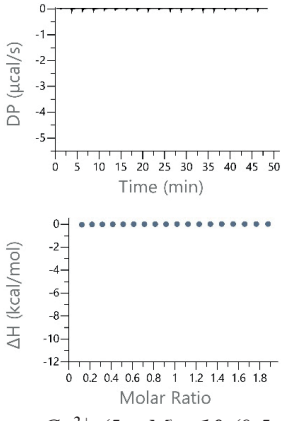

*Ca^{2+} (5 mM) : **10** (0.5 mM)*

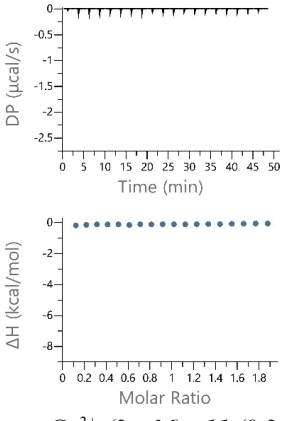

*Ca^{2+} (2 mM) : **11** (0.2 mM)*

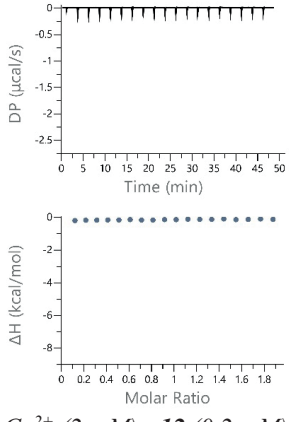

*Ca^{2+} (2 mM) : **12** (0.2 mM)*

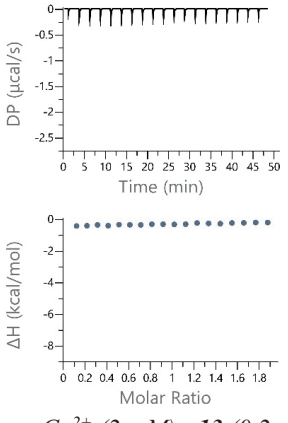

*Ca^{2+} (2 mM) : **13** (0.2 mM)*

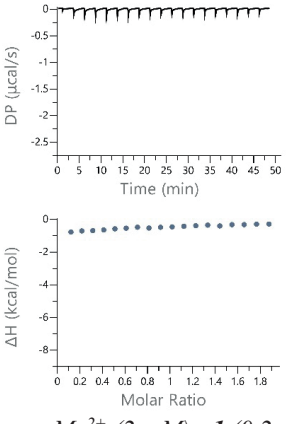

*Mg^{2+} (2 mM) : **1** (0.2 mM)*

Figure S2. *continued*

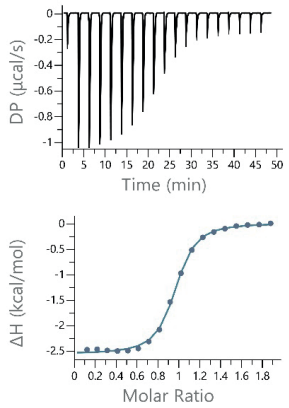

*Mg^{2+} (2 mM) : **2** (0.2 mM)*

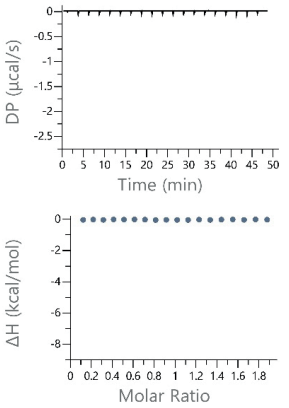

*Mg^{2+} (2 mM) : **3** (0.2 mM)*

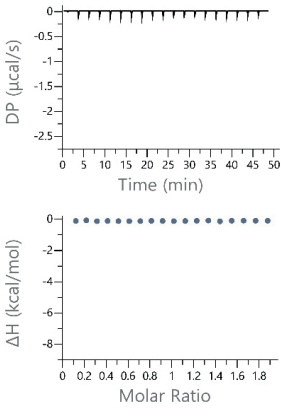

*Mg^{2+} (2 mM) : **4** (0.2 mM)*

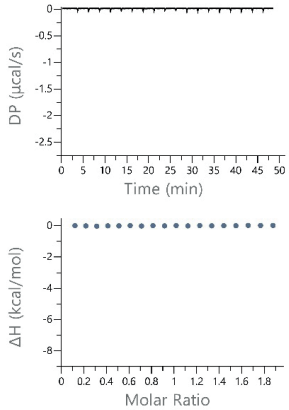

*Mg^{2+} (2 mM) : **5** (0.2 mM)*

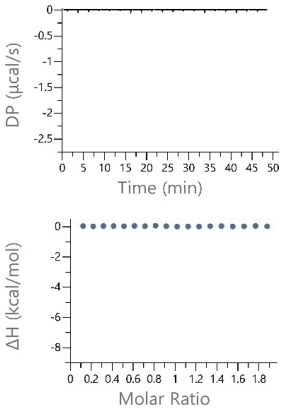

*Mg^{2+} (2 mM) : **6** (0.2 mM)*

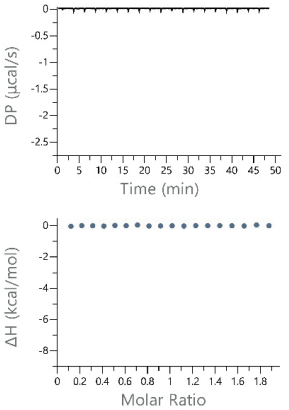

Mg^{2+} (2 mM) : 7 (0.2 mM)

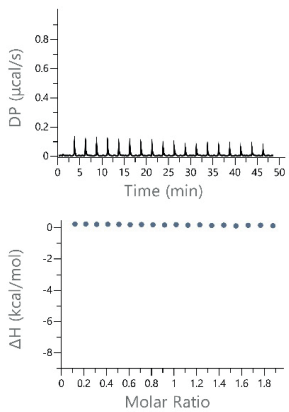

*Mg^{2+} (2 mM) : **8** (0.2 mM)*

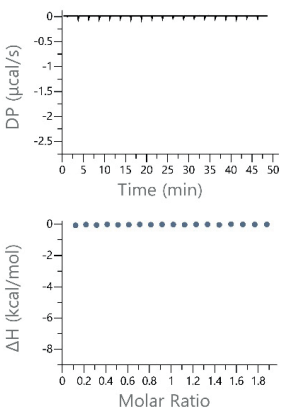

*Mg^{2+} (2 mM) : **9** (0.2 mM*

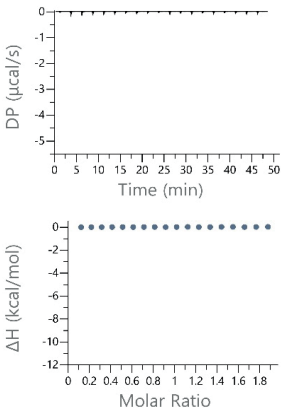

*Mg^{2+} (5 mM) : **8** (0.5 mM)*

Figure S2. *continued*

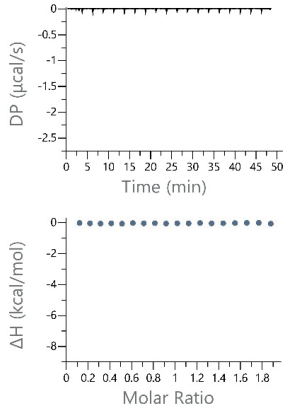

*Mg^{2+} (2 mM) : **11** (0.2 mM)*

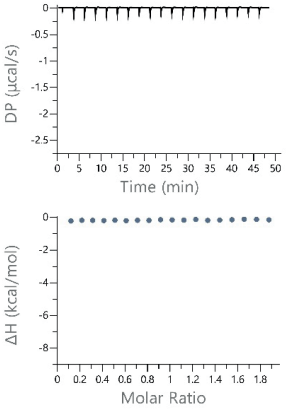

*Mg^{2+} (2 mM) : **12** (0.2 mM)*

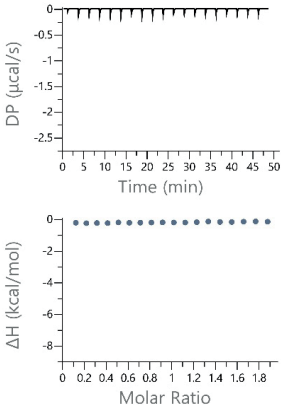

*Mg^{2+} (2 mM) : **13** (0.2 mM)*

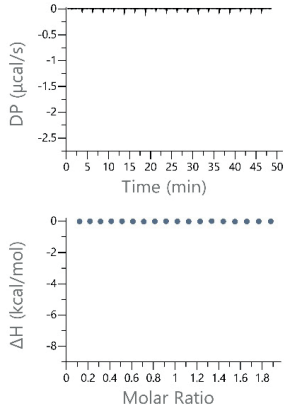

*Buffer : **1** (0.2 mM)*

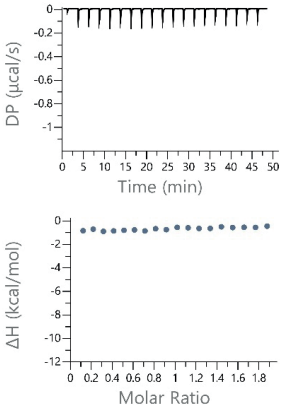

*Buffer : **1** (0.05 mM)*

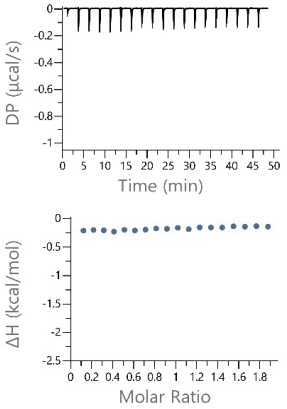

*Buffer : **2** (0.2 mM)*

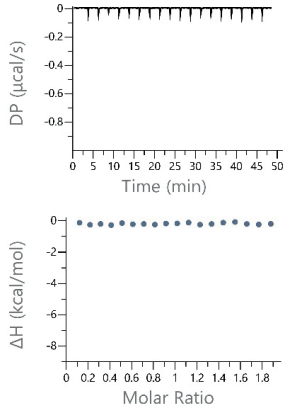

*Buffer : **2** (0.05 mM)*

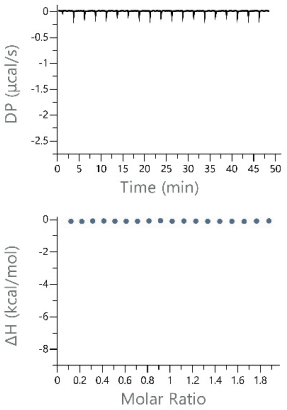

*Buffer : **3** (0.2 mM)*

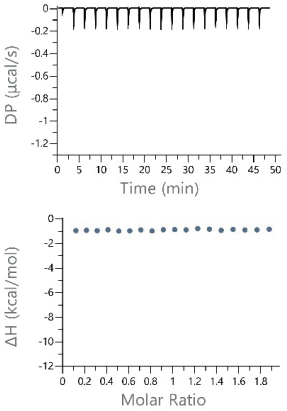

*Buffer : **3** (0.05 mM)*

Figure S2. *continued*

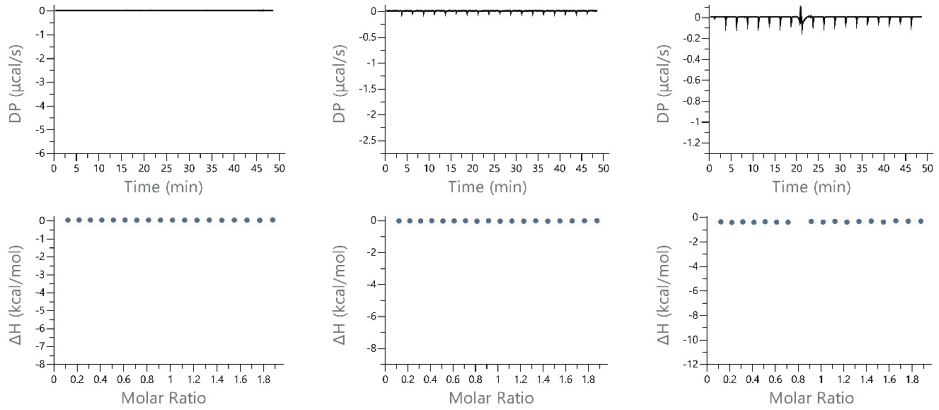

*Buffer : **4** (0.5 mM)* *Buffer : **4** (0.2 mM)* *Buffer : **4** (0.05 mM)*

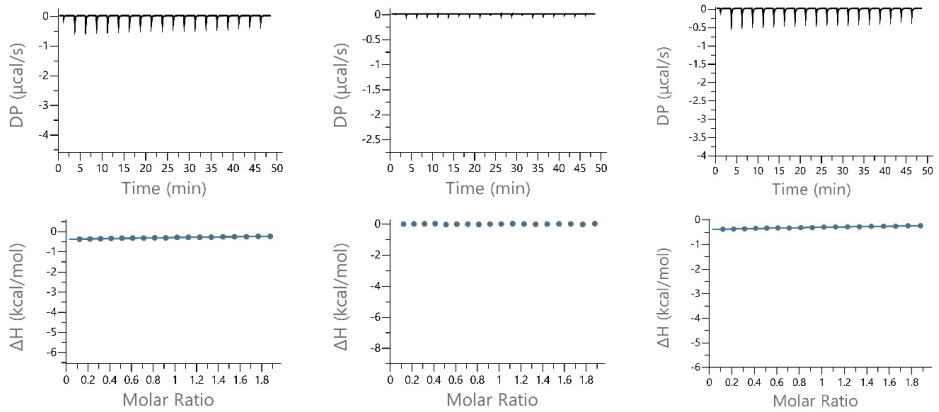

*Buffer : **5** (0.5 mM)* *Buffer : **5** (0.2 mM)* *Buffer : **6** (0.5 mM)*

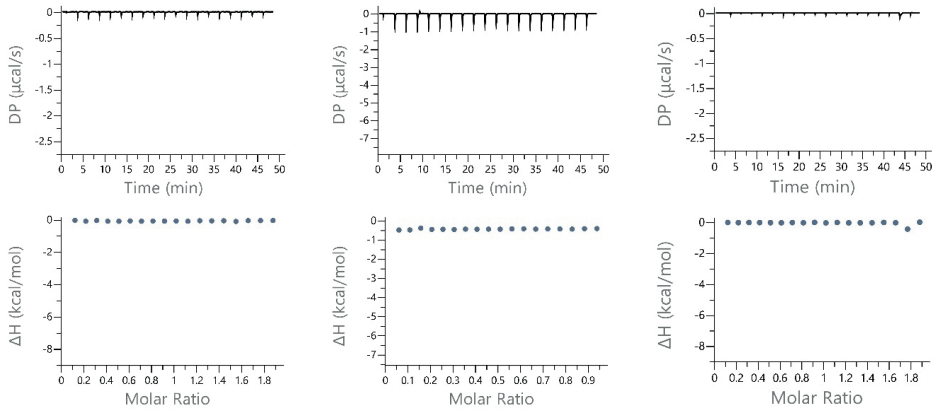

*Buffer : **6** (0.2 mM)* *Buffer : **7** (1 mM)* *Buffer : **7** (0.2 mM)*

Figure S2. *continued*

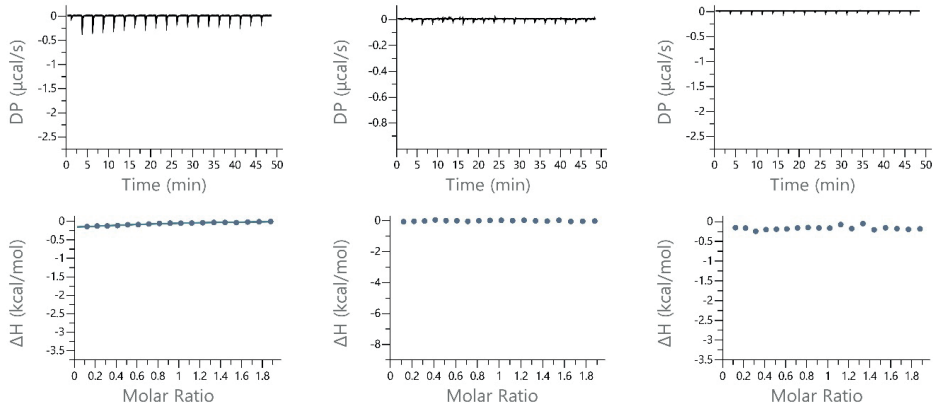

*Buffer : **8** (0.5 mM)* *Buffer : **8** (0.2 mM)* *Buffer : **8** (0.05 mM)*

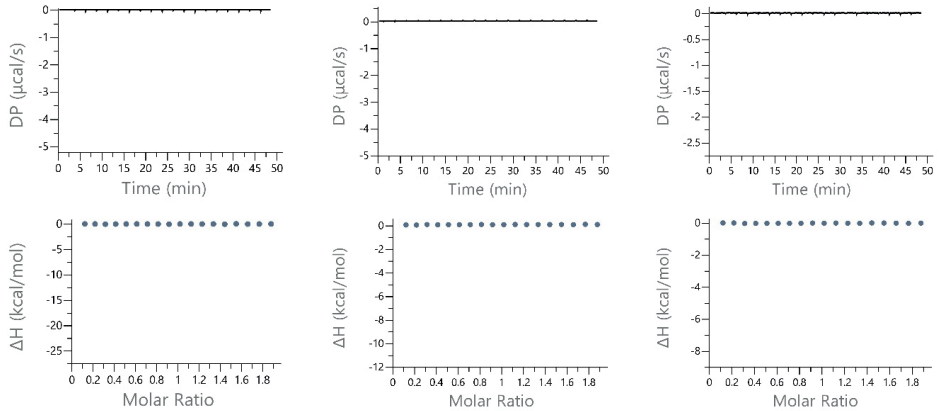

*Buffer : **9** (0.2 mM)* *Buffer : **10** (0.5 mM)* *Buffer : **11** (0.2 mM)*

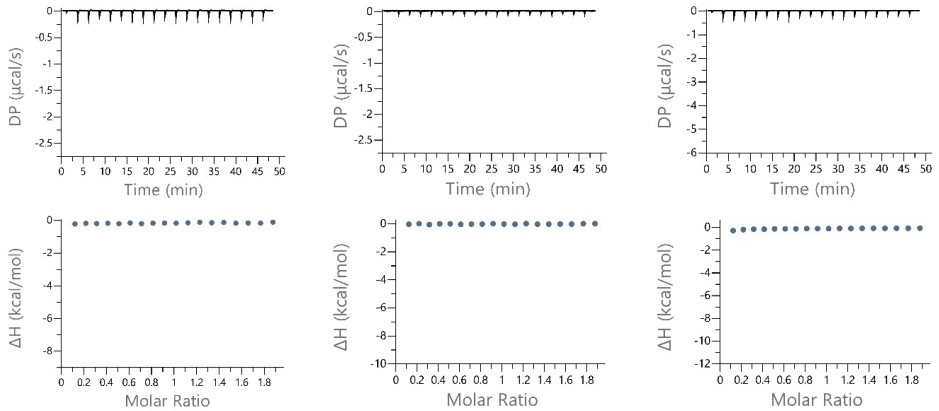

*Buffer : **12** (0.2 mM)* *Buffer : **13** (0.2 mM)* *Zn^{2+} (5 mM) : Buffer*

Figure S2. *continued*

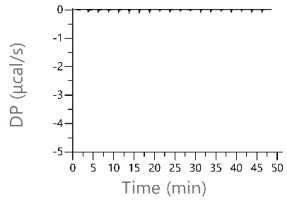

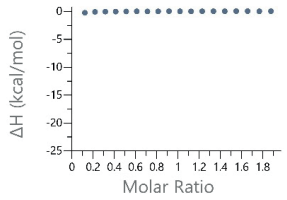

Zn^{2+} (2 mM) : Buffer

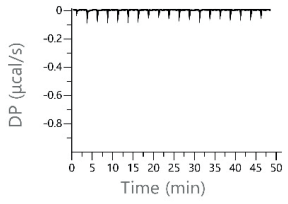

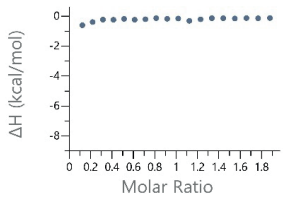

Zn^{2+} (0.5 mM) : Buffer

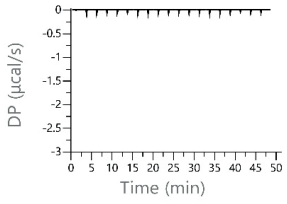

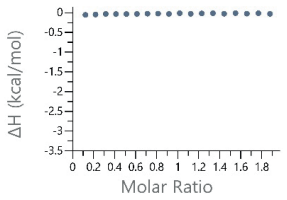

Ca^{2+} (5 mM) : Buffer

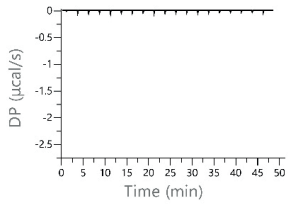

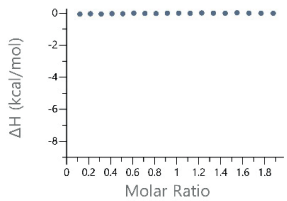

Ca^{2+} (2mM) : Buffer

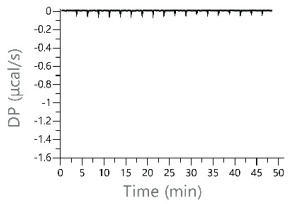

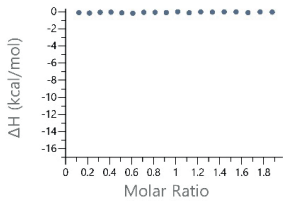

Ca^{2+} (0.5 mM) : Buffer

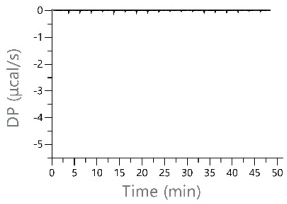

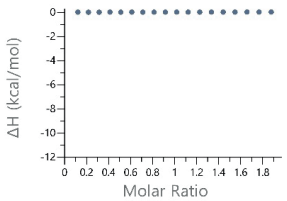

Mg^{2+} (5 mM) : Buffer

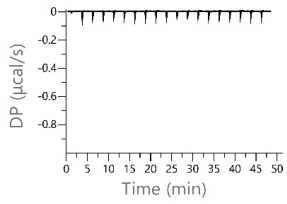

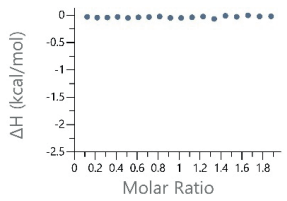

Mg^{2+} (2 mM) : Buffer

Figure S2. *continued*

Table S3. MIC values for MBL inhibitors studied and meropenem against NDM-1 expressing *E. coli* isolate.

Compound	MIC values[a] against *E. coli RC89* (NDM-1)
1	>2000
2	>2000
3	>2000
4	125
5	1000
6	>2000
7	>2000
8	>2000
9	>2000
10	>2000
11	>2000
12	>2000
13	>2000
Meropenem	167 (corresponds to 64 μg/mL)

[a]MIC values given in μM

6. References

1 T. P. Van Boeckel, S. Gandra, A. Ashok, Q. Caudron, B. T. Grenfell, S. A. Levin and R. Laxminarayan, *Lancet Infect. Dis.*, 2014, **14**, 742–750.

2 S. M. Drawz and R. A. Bonomo, *Clin. Microbiol. Rev.*, 2010, **23**, 160–201.

3 R. P. Ambler, *Philos. Trans. R. Soc. London B*, 1980, **289**, 321–331.

4 D. de A. Viana Marques, S. E. F. Machado, V. Carvalho Santos Ebinuma, C. de A. L. Duarte, A. Converti and A. L. F. Porto, *Antibiotics*, 2018, **7**, 1–26.

5 H. Feng, J. Ding, D. Zhu, X. Liu, X. Xu, Y. Zhang, S. Zang, D. C. Wang and W. Liu, *J. Am. Chem. Soc.*, 2014, **136**, 14694–14697.

6 V. L. Green, A. Verma, R. J. Owens, S. E. V. Phillips and S. B. Carr, *Acta Crystallogr. Sect. F Struct. Biol. Cryst. Commun.*, 2011, **67**, 1160–1164.

7 N. O. Concha, C. A. Janson, P. Rowling, S. Pearson, C. A. Cheever, B. P. Clarke, C. Lewis, M. Galleni, J. M. Frère, D. J. Payne, J. H. Bateson and S. S. Abdel-Meguid, *Biochemistry*, 2000, **39**, 4288–4298.

8 H. Zhang and Q. Hao, *FASEB J.*, 2011, **25**, 2574–2582.

9 D. Yong, M. A. Toleman, C. G. Giske, H. S. Cho, K. Sundman, K. Lee and T. R. Walsh, *Antimicrob. Agents Chemother.*, 2009, **53**, 5046–5054.

10 T. Li, Q. Wang, F. Chen, X. Li, S. Luo, H. Fang, D. Wang, Z. Li, X. Hou and H. Wang, *PLoS One*, 2013, **8**, 1–5.

11 N. Laraki, N. Franceschini, G. M. Rossolini, P. Santucci, C. Meunier, E. De Pauw, G. Amicosante, J. M. Frère and M. Galleni, *Antimicrob. Agents Chemother.*, 1999, **43**, 902–906.

12 L. C. Ju, Z. Cheng, W. Fast, R. A. Bonomo and M. W. Crowder, *Trends Pharmacol. Sci.*, 2018, **39**, 635–647.

13 A. M. King, S. A. Reid-Yu, W. Wang, D. T. King, G. De Pascale, N. C. Strynadka, T. R. Walsh, B. K. Coombes and G. D. Wright, *Nature*, 2014, **510**, 503–506.

14 D. T. King, L. J. Worrall, R. Gruninger and N. C. J. Strynadka, *J. Am. Chem. Soc.*, 2012, **134**, 11362–11365.

15 A. J. Turner, in *The Protective Arm of the Renin Angiotensin System (RAS): Functional Aspects and Therapeutic Implications*, Elsevier Inc., 2015, pp. 185–189.

16 A. J. Baxter and E. P. Krenzelok, *Clin. Toxicol.*, 2008, **46**, 1083–1084.

17 B. M. R. Liénard, G. Garau, L. Horsfall, A. I. Karsisiotis, C. Damblon, P. Lassaux, C. Papamicael, G. C. K. Roberts, M. Galleni, O. Dideberg, J. M. Frère and C. J.

Schofield, *Org. Biomol. Chem.*, 2008, **6**, 2282–2294.

18 K. H. M. E. Tehrani and N. I. Martin, *ACS Infect. Dis.*, 2017, **3**, 711–717.

19 P. W. Lee, H. Aizawa, L. L. Gan, C. Praksha and D. Zhong, Eds., in *Handbook of Metabolic PAthways of Xenobiotics*, John Wiley & Sons, 2014, pp. 1–3.

20 A. M. Somboro, D. Tiwari, L. A. Bester, R. Parboosing, L. Chonco, H. G. Kruger, P. I. Arvidsson, T. Govender, T. Naicker and S. Y. Essack, *J. Antimicrob. Chemother.*, 2014, **70**, 1594–1596.

21 R. Azumah, J. Dutta, A. M. Somboro, M. Ramtahal, L. Chonco, R. Parboosing, L. A. Bester, H. G. Kruger, T. Naicker, S. Y. Essack and T. Govender, *J. Appl. Microbiol.*, 2016, **120**, 860–867.

22 Q. Wang, Y. He, R. Lu, W. M. Wang, K. W. Yang, H. M. Fan, Y. Jin and G. Michael Blackburn, *Biosci. Rep.*, 2018, **38**, 1–11.

23 L. E. Horsfall, G. Garau, B. M. R. Liénard, O. Dideberg, C. J. Schofield, J. M. Frère and M. Galleni, *Antimicrob. Agents Chemother.*, 2007, **51**, 2136–2142.

24 F. M. Klingler, T. A. Wichelhaus, D. Frank, J. Cuesta-Bernal, J. El-Delik, H. F. Müller, H. Sjuts, S. Göttig, A. Koenigs, K. M. Pos, D. Pogoryelov and E. Proschak, *J. Med. Chem.*, 2015, **58**, 3626–3630.

25 C. Mollard, C. Moali, C. Papamicael, C. Damblon, S. Vessilier, G. Amicosante, C. J. Schofield, M. Galleni, J. M. Frère and G. C. K. Roberts, *J. Biol. Chem.*, 2001, **276**, 45015–45023.

26 N. Li, Y. Xu, Q. Xia, C. Bai, T. Wang, L. Wang, D. He, N. Xie, L. Li, J. Wang, H. G. Zhou, F. Xu, C. Yang, Q. Zhang, Z. Yin, Y. Guo and Y. Chen, *Bioorganic Med. Chem. Lett.*, 2014, **24**, 386–389.

27 W. S. Shin, A. Bergstrom, J. Xie, R. A. Bonomo, W. Michael, R. Muthyala, Y. Y. Sham, C. Pharmacology and C. B. Program, *ChemMedChem*, 2017, **12**, 845–849.

28 WO/2017/093727, 2017, 171.

29 WO/2014/198849, 2014, 172.

30 S. Leiris, A. Coelho, J. Castandet, M. Bayet, C. Lozano, J. Bougnon, J. Bousquet, M. Everett, M. Lemonnier, N. Sprynski, M. Zalacain, T. D. Pallin, M. C. Cramp, N. Jennings, G. Raphy, M. W. Jones, R. Pattipati, B. Shankar, R. Sivasubrahmanyam, A. K. Soodhagani, R. R. Juventhala, N. Pottabathini, S. Pothukanuri, M. Benvenuti, C. Pozzi, S. Mangani, F. De Luca, G. Cerboni, J. D. Docquier and D. T. Davies, *ACS Infect. Dis.*, 2019, **5**, 131–140.

31 C. A. Thomas, Z. Cheng, K. Yang, E. Hellwarth, C. J. Yurkiewicz, F. M. Baxter, S. A.

Fullington, S. A. Klinsky, J. L. Otto, A. Y. Chen, S. M. Cohen and M. W. Crowder, *J. Inorg. Biochem.*, 2020, **210**, 111–123.

32 S. S. Van Berkel, J. Brem, A. M. Rydzik, R. Salimraj, R. Cain, A. Verma, R. J. Owens, C. W. G. Fishwick, J. Spencer and C. J. Schofield, *J. Med. Chem.*, 2013, **56**, 6945–6953.

33 K. H. M. E. Tehrani, H. Fu, N. C. Brüchle, V. Mashayekhi, A. Prats Luján, M. J. Van Haren, G. J. Poelarends and N. I. Martin, *Chem. Commun.*, 2020, **56**, 3047–3049.

34 S. Minisola, J. Pepe, S. Piemonte and C. Cipriani, *BMJ*, 2015, **350**, 1–9.

35 J. Soar, G. D. Perkins, G. Abbas, A. Alfonzo, A. Barelli, J. J. L. M. Bierens, H. Brugger, C. D. Deakin, J. Dunning, M. Georgiou, A. J. Handley, D. J. Lockey, P. Paal, C. Sandroni, K. C. Thies, D. A. Zideman and J. P. Nolan, *Resuscitation*, 2010, **81**, 1400–1433.

36 A. Krężel and W. Maret, *Arch. Biochem. Biophys.*, 2016, **611**, 3–19.

37 K. Jeong, C. C. Slack, C. C. Vassiliou, P. Dao, M. D. Gomes, D. J. Kennedy, A. E. Truxal, L. J. Sperling, M. B. Francis, D. E. Wemmer and A. Pines, *ChemPhysChem*, 2015, **16**, 3573–3577.

38 G. Anderegg, E. Hubmann, N. G. Podder and F. Wenk, *Helv. Chim. Acta*, 1977, **60**, 123–140.

39 O. Jøns and E. S. Johansen, *Inorganica Chim. Acta*, 1988, **151**, 129–132.

40 L. Chung, K. S. Rajan, E. Merdinger and N. Grecz, *Biophys. J.*, 1971, **11**, 469–482.

41 M. A. Hughes, G. L. Smith and D. R. Williams, *Inorganica Chim. Acta*, 1985, **7**, 247–252.

42 S. Fullington, Z. Cheng, C. Thomas, C. Miller, K. Yang, L. C. Ju, A. Bergstrom, B. A. Shurina, S. L. Bretz, R. C. Page, D. L. Tierney and M. W. Crowder, *J. Biol. Inorg. Chem.*, 2020, **25**, 717–727.

43 D. H. Griffin, T. K. Richmond, C. Sanchez, A. J. Moller, R. M. Breece, D. L. Tierney, B. Bennett and M. W. Crowder, *Biochemistry*, 2011, **50**, 9125–9134.

44 K. H. M. E. Tehrani, N. C. Brüchle, N. Wade, V. Mashayekhi, D. Pesce, M. J. van Haren and N. I. Martin, *ACS Infect. Dis.*, 2020, **6**, 1366–1371.